Cancer Chemother Pharmacol (2006) 58: 245–255
DOI 10.1007/s00280-005-0145-x

ORIGINAL ARTICLE

**Siqing Shan · Clay Flowers · Cathy D. Peltz
Heather Sweet · Norbert Maurer · Eun-Joo Gina Kwon
Ave Krol · Fan Yuan · Mark W. Dewhirst**

# Preferential extravasation and accumulation of liposomal vincristine in tumor comparing to normal tissue enhances antitumor activity

Received: 29 July 2005 / Accepted: 12 October 2005 / Published online: 8 December 2005


**Abstract** To quantitatively evaluate the extravasation, accumulation and selectivity to tumor tissues of liposomal vincristine (LV), dorsal skin-fold window chambers on athymic mice with or without LX-1, a human small cell lung cancer, xenograft implants and fluorescent intravital microscopy imaging were used. In vitro studies show that minimal loss of fluorescence marker DiI from liposomes occurs after 4 days of inoculation in murine plasma, and the release profiles of DiI-LV and LV were essentially the same with approximately 40% of the encapsulated vincristine sulfate (VCR) released after 26 h. Significantly faster extravasation of DiI-LV from tumor vessels was shown compared to non-tumor tissue after single dose i.v. administration. The relative interstitial amounts at 60 min ($RIA_{60}$) for tumor and non-tumor tissues were $0.837 \pm 0.314$ and $0.012 \pm 0.091$, respectively ($P = 0.01$). DiI-LV accumulation was significantly higher in tumor than in normal tissue, which continued beyond 48 h. Both DiI-LV and LV showed significant antitumor effects in window chambers and in flank tumors, compared with controls and VLS alone. The preferential extravasation of DiI-LV from tumor vasculature as well as its differential retention in tumor tissue provides the basis for the enhancement in antitumor activity of LV over VCR.

S. Shan · C. D. Peltz · M. W. Dewhirst (✉)
Department of Radiation Oncology,
Duke University Medical Center,
201 Med. Sci. Res. Bldg., Box 3455, Durham,
NC 27710, USA
E-mail: dewhirst@radonc.duke.edu
Tel.: +1-919-6848400
Fax: +1-919-6848718

A. Krol · F. Yuan
Department of Biomedical Engineering,
Duke University, Durham, NC 27710, USA

C. Flowers · H. Sweet · N. Maurer · E.-J. G. Kwon
Inex Pharmaceuticals Corporation, Glenyon Parkway,
V5J 5J8, Burnaby, BC, Canada

**Keywords** Vincristine · Liposome · Fluorescence microscopy · Extravasation · Drug release · Dorsal skin fold window chamber · LX-1 human small cell lung cancer

## Introduction

Liposomal drug delivery systems have demonstrated the capacity to alter the pharmacokinetics and biodistribution of conventional chemotherapeutic drugs with the goal of increasing efficacy or reducing toxicity [1–4]. Classes of cytotoxic drugs encapsulated into liposomes and tested in humans include anthracyclines, pyrimidine analogs, and vinca alkaloids [5, 6]. The anthracyclines are schedule-independent cytotoxic drugs in which efficacy and toxicity are associated with high peak levels of drug in tumor tissues or target organs. Liposomal doxorubicin decreased systemic elimination, increased penetration into the tumor, and prolonged liposome presence with slow drug release into the tumor, and thus enhanced therapeutic effect [7, 8]. In patients, the use of liposomal delivery system allows for an increased total cumulative dose due to decreased cardiotoxicity [9].

In contrast to the anthracyclines, the vinca alkaloids are schedule-dependent drugs with activity dependent on binding to tubulin, inhibiting the formation of mitotic spindles, resulting in cell cycle arrest and apoptosis [10]. Therefore, the degree of antitumor activity of vincristine in cell is directly related to the duration of drug exposure of tumor cells. However, conventional vincristine is rapidly removed from the systemic circulation following i.v. administration. Efforts to enhance vincristine activity in patients included clinical trials using continuous drug infusion but these studies evaluated a limited number of patients and the results were inconclusive [10, 11].

Liposomal vincristine (LV) was designed to enhance the antitumor activity of vincristine via the following mechanisms: (1) increased plasma circulation time; (2) increased drug delivery to the tumor tissue via extravasation from abnormal tumor vessels into the tumor

interstitium; (3) accumulation of liposomes containing drug in the tumor tissues; and (4) slow release of vincristine from LV in tumors as opposed to release of drug in plasma favors maximizing exposure. Previous studies in mice demonstrated that LV exhibits prolonged plasma circulation and increased tumor accumulation compared to equivalent doses of vincristine sulphate (VCR) [12, 13]. The altered pharmacokinetic profile of LV was associated with significantly greater antitumor activity in murine and human xenograft tumor models relative to vincristine when compared at the same dose level [12, 14–19]. A recent study shows that LV sensitizes drug-resistant human tumor xenografts in the mouse [20].

In this report, the extravasation of LV from blood vessels into tissues was evaluated with regards to kinetics, accumulation, and selectivity. Intravital microscopy and skin fold window chambers in mice were employed to study the extravasation and tissue distribution of LV labeled with a fluorescent lipid marker, 1,1′-dioctadecyl-3, 3,3′, 3′-tetramethylindocarbocyanine perchlorate (DiI-LV). Using the same tumor model as employed for the window chamber studies, the antitumor activity of LV was compared with vincristine in tumors transplanted subcutaneously on the hindlimbs.

## Materials and methods

### Chemicals and reagents

Egg sphingomyelin was obtained from Lipoid (Ludgwighafen, Germany), cholesterol from Solvay (Weesp, The Netherlands), DiI from Molecular Probes (Eugene, OR), VCR from Faulding Pharmaceuticals (Paramus, NJ), Dulbecco's Phosphate Buffered Saline (DPBS) from Gibco BRL (Grand Island, NY). Sepharose CL-6B and Sepharose CL-4B were from Sigma (St. Louis, MO), PD-10 columns from Amersham Biosciences (Piscataway, NJ), $^{3}$H-CHE from PerkinElmer Life Sciences (Boston MA), $^{14}$C-labeled vincristine from ChemSyn Laboratories (Lenexa, Kansas), and Nuclepore extrusion filters from Whatman (Clifton, NJ).

### Liposome preparation

Sphingomyelin/cholesterol (55/45) liposomes were prepared through hydration of the lipids from ethanol. The final ethanol concentration was 12.5% (w/w) and the lipid concentration was 15 mg/ml. The ethanolic lipid dispersions were extruded 10 × at 65°C through two stacked nuclepore filters with 80 nm pore size. Ethanol was removed by dialysis for a total of 24 h against citrate buffer (pH 4.0). DiI was dissolved with the other lipids in ethanol prior to liposome formation. DiI-LV contained 0.5 mol% DiI. Lipid concentrations were determined using the inorganic phosphorus assay according to Fiske and Subbarow [21]. These diameters were determined through a Gaussian fit to the measured intensity correlation functions. The average diameter of the liposomes was between 100 and 110 nm.

### Vincristine loading

Liposomes were loaded with VCR using a pH gradient technique [18]. Briefly, liposomes were prepared in pH 4 citrate buffer. The exterior pH of the liposomes was then raised to pH 7.3 through addition of 0.1 M $Na_2HPO_4$ solution (pH 9.0). Alternatively, buffer neutralization was achieved by exchanging the citrate buffer on PD-10 buffer exchange columns against pH 7.3 phosphate buffer (100 mM phosphate buffer [pH 9] adjusted to pH 7.3 with 300 mM citrate buffer [pH 4]). VCR alone or spiked with $^{14}$C-labeled vincristine was subsequently added to the various liposome formulations to achieve a drug-to-lipid ratio of 0.05 mg/mg (0.03 mol/mol) and a $^{14}$C-vincristine-to-$^{3}$H-CHE radioactivity ratio of approximately 3. The mixture was subsequently incubated for 10 min at 63°C. The final vincristine concentration in the loaded sample was 0.16 mg/ml (0.17 mM).

Encapsulation efficiencies were determined after removal of external drug by size exclusion chromatography using Sepharose CL-6B spin columns equilibrated in DPBS [22]. Vincristine concentrations were determined by UV absorption at 297 nm in 80% ethanol and lipid concentrations using the inorganic phosphorus assay according to Fiske and Subbarow [21].

### Vincristine release in mouse plasma in vitro

The plasma was obtained from ketamine/xylazine anesthetized NCr-nu athymic mice via cardiac puncture and centrifugation. Frozen plasma aliquots were thawed and adjusted to pH 7.4 through addition of 1 M HEPES buffer. Liposomes were then added to the plasma to achieve a final lipid concentration of 0.6 mg/ml (1.1 mM). Samples were incubated in a water bath at 37°C. At the given time points, 100 µl aliquots were removed and put on Sepharose CL-6B spin columns and centrifuged for 5 min at 960*g* to separate free from encapsulated vincristine. Encapsulated drug levels were determined by dual-label scintillation counting.

### Dissociation of DiI from SM/Ch liposome in mouse plasma in vitro

Frozen mouse plasma was thawed and buffered to pH 7.4 as mentioned previously. Liposomes were then added to the plasma at a final lipid concentration of 0.6 mg/ml (1.1 mM). Samples were incubated at 37°C. After 24 and 96 h, 900 µl sample aliquots were removed and separated on a 1.5 × 40 cm Sepharose CL-4B size exclusion column equilibrated in DPBS. The size exclusion columns were pre-saturated with unlabeled

liposomes to maximize recoveries. The column was protected from light to prevent bleaching of DiI. The fractions with approximately 550 μl each were analyzed for DiI fluorescence with the excitation set at 550 nm and collecting emitted light at 565 nm. Liposomes incubated in DPBS at 37°C for 24 h and unlabeled liposomes mixed with free DiI incubated in plasma at 37°C for 24 h were included as controls.

## Tumor and animals

The human small cell lung cancer line, LX-1 (NCI Tumor Repository, Rockville, MD), was injected s.c. into the flanks of 6–8 week-old NCr-nu athymic mice (Charles River Laboratory, Raleigh, NC). This xenograft model is one of a panel of tumor models employed by the NCI in the evaluation of potential chemotherapeutic agents [23]. Historical data on LX-1 suggests that the model is relatively resistant to VCR [24]. Animals were housed in appropriate isolated caging with sterile rodent chow and acidified water ad libitum and an air-conditioned room with 12-h light-dark cycle. All experimental protocols were approved by the Duke Institutional Animal Care and Use Committee.

## Dorsal skin fold window chamber

The surgical procedure for the mouse dorsal skin fold window chamber has been reported previously [25]. Briefly, animals were anesthetized with i.p. sodium pentobarbital (Nembutal, Abbott Laboratory) at a dose of 85 mg/kg. With aseptic technique, a circular incision of 10 mm diameter was made on the left side of the flap and a full-thickness skin layer was removed, leaving the skin and underlying fascia tissue on the right side intact. A pair of titanium windows was mounted with alignment of the circular wound to the window, which was covered with a glass cover slip and a retaining ring after LX-1 tumor fragment (about 0.1 $mm^3$) was implanted onto the fascia. Following recovery from anesthesia and surgery, the animals were housed in an environmental chamber at 35°C and 50% humidity, with 12-h light/12-h dark cycle and access to rodent chow and water ad libitum. These conditions are necessary to maintain viability of the chamber and provide a high enough temperature to facilitate tumor growth.

## Experimental protocol

From post-operative day (POD)4 tumor growth in the window chambers was monitored with intravital microscopy (Carl Zeiss, Hanover, MD) with a CCD camera (Carl Zeiss, Inc) connected to a PC equipped with Scion Image software and a frame grabber (Scion Corporation, Frederick, MD). Before treatment, window chambers were evaluated for quality and tumors were scored using criteria for tumor size, vasculature, blood flow, as reported previously [26]. It has been shown previously that this quality assurance procedure ensures that a viable tumor is established before the experiment commences. For study of extravasation of DiI-LV in normal granulation tissue, non-tumor-bearing windows were used on POD 5 and 7. Forty mice were used in this study (32 tumor-bearing and 8 non-tumor-bearing). There were four study groups: 11 tumor-bearing mice for DiI-LV extravasation, 12 tumor-bearing mice were treated with LV for comparison with Dil-LV, 8 tumor-free mice for DiI-LV extravasation in normal granulation tissue, and 9 mice treated with 0.9% NaCl solution as control. The vincristine dose for LV and DiI-LV was 1.6 mg/kg. The dose selected for this study was based on a maximum tolerated dose study in tumor-free NCr-nu athymic mice (data not shown).

## Effects of LV and DiI-LV on tumor growth and angiogenesis in the dorsal skin chamber

Tumors in the dorsal window chambers were monitored serially after liposome administration to assess the effect of this treatment on tumor growth and angiogenesis. For consistency with DiI-LV extravasation experiments that require strict restraint with general anesthesia, LV was given while animals were anesthetized with Nembutal (50 mg/kg). Anesthetized controls received the same amount of sterile 0.9% NaCl solution. For measurement of tumor area and vascular length density as the experimental endpoints, animals were placed on a Zeiss intravital microscope stage and trans-illuminated images were taken on post-treatment day (PTD) 0, 2, 5, and 8 using a CCD color camera (Carl Zeiss, Inc.). Images were captured and analyzed using Scion Image software (Scion Corporation). PTD 8 was chosen as the day for termination because tumors in all control mice receiving 0.9% NaCl solution grew beyond the window margins at this time point. The detailed methods for quantitation of tumor growth and vasculature were reported previously [26]. Tumor area was measured from images at low magnification and converted to $mm^2$ by calibration against images of a micrometer obtained at the same magnification. Vascular length density (VLD) was measured from 1 to 4 images from different areas of tumors, depending on tumor size, at higher magnification. All vessels were traced and measured. Total vessel length in each image was summed and the area containing the measured vessels was also measured. VLD was calculated by dividing the total length of all vessels by the tumor area and expressed as $mm/mm^2$.

## Dil-LV extravasation and tissue distribution in tumor and non-tumor windows

On POD 5 or POD 7, mice with non-tumor-bearing windows were used for Dil-LV extravasation experiments.

For tumor-bearing mice, experiments were carried out on POD 7 or POD 9. Before administration of DiI-LV, animals were anesthetized with Nembutal (50 mg/kg i.p) and the tail vein was cannulated with a 31G needle with PE10 tubing and heparinized 0.9% NaCl solution-filled syringe attached. Animals were placed on a thermal blanket (Harvard Homeothermic Blanket Control Unit, Harvard Apparatus, Lit., Edenbridge, KY), which was located on the stage of the Zeiss intravital microscope. Under transillumination, an area with well-focused vessels and brisk blood flow was chosen for the experiment. Before Dil-LV injection a background image with a rhodamine filter set (excitation 545 nm and emission 610 nm) was taken with a SIT camera (Hamamatsu, C2400-08) connected to an image processor (Hamamatsu Image Processor Argus, Hamamatzu Photonics) and videocassette recorder (JVC BR-S378U). Epi-illumination was provided with an arc lamp (AttoArc HBO 100W, Carl Zeiss, Inc) with adjustable power level. Dil-LV (1.6 mg VCR/kg, in the volume of 10 μl/g body weight) was injected over 2–3 min, and the serial images were tape-recorded and captured to Scion Image every 2 min after injection for 60 min.

The images were analyzed with NIH Image 1.62. The fluorescent light intensities of the entire selected region and representative vascular regions were measured at each serial time point. The background value was subtracted from all measurements. The relative fluorescent light intensities of the vascular and interstitial components were determined as described previously [27, 28]. All light intensities were normalized to the initial vascular light intensity in the region after injection of Dil-LV. Since the light intensity of fluorescent tracers is proportional to the number of fluorophores present, the data are presented as relative interstitial amount (RIA) as reported previously [27]. RIA is the average fluorescent intensity in the tumor interstitium, compared with maximum intravascular intensity after fluorescent marker administration. RIA values taken at 60 min are defined as $RIA_{60}$.

Following the initial extravasation measurements, the animals were returned to their housing. They were re-imaged, without anesthesia, at 16, 24, and 48 h after drug injection. These data were used for quantitation of tissue distribution. Some fluorescence microscopic images of tumor windows were recorded on PTD 5. Fluorescent light intensities were also measured from images taken in three to four areas in tumor and surrounding normal tissue, respectively, using the same magnification and light power levels used prior to Dil-LV injection on PTD 0. These data were used to calculate average light intensities in tumor tissue and surrounding tissue at 16, 24, and 48 h post-injection. During the intervals between imaging procedures, the window chambers were wrapped with aluminum foil to minimize photobleaching of fluorescent dye. Trans-illumination images of tumor windows were also recorded on PTD 0, 2, 5, and 8 after Dil-LV injection to evaluate tumor growth and vascular density as described earlier for LV.

### Comparison of the antitumor activity of LV and VCR in mice bearing LX-1 tumors

On Day 0, LX-1 tumor fragments (14–17 mg) were implanted s.c. in the right hind flank of Halothane-anesthetized mice using a 10 G trocar. When the tumors reached tumor volumes of $\sim$20 $mm^3$, drugs were injected i.v. every 7 days for three consecutive cycles. Tumors were measured twice a week and tumor volume was calculated using the equation for the volume of an ellipse: $1/6\pi LWH$. Antitumor activity of LV and VCR was evaluated by comparing tumor volumes on specified days and by determining the time for tumors to attain a volume of 1,000 $mm^3$.

### Quantification of available volume fraction of inulin in tumor tissues

The available volume fraction ($K_{AV}$) of inulin (mol wt: 2,000–5,000) in the tumor was determined with the procedure described in previous studies [29–31]. In brief, tumor tissue slices were incubated in the solution of FITC-labeled inulin in microcentrifuge tubes at 4°C until concentration equilibrium was reached between slices and solutions. Next, tissue slices and the solution were transferred into circular wells glued onto the surface of glass microslides. The well height was $h_{well}$. Fluorescence intensities after background subtraction in tissues ($\Delta I_t$) and solution ($\Delta I_{sol}$) were measured separately in the wells, using a fluorescence microscope workstation (Axiovert 100, Zeiss) equipped with a fluorescence filter set for FITC (Omega Optical Inc., Brattleboro, VT) and a photomultiplier (9658B, Thorn EMI Electron Tubes, Rockaway, NJ). $K_{AV}$ was calculated based on the fluorescence intensities,

$$K_{AV} = \alpha h_{well} \frac{\Delta I_t}{\Delta I_{sol}},$$

where $\alpha$ is a constant that depends on fluorescent markers and optical properties of tissues. For FITC in tumor tissues, $\alpha = 3.02(\pm 1.34\ mm^{-1}$ [29].

### Statistics

All results are reported as group means and SEMs. Statistical significance was tested by the Student's two-tailed unpaired *t*-test.

## Results

### Stability of DiI labeling and VCR release from DiI-LV

Following incubation of DiI-LV in murine plasma for 24 h, 6.5% of the fluorescent marker was dissociated from the liposomes. After 96 h of incubation, 11.5% of

DiI was separated from the liposomes. Incubation of DiI-LV in 0.9% NaCl solution showed that all of the DiI remained with the liposomes after 96 h of incubation suggesting that DiI-LV is stable after administration and the slow disassociation of DiI from LV occurs beyond the time period of the quantitative observation in vivo.

To test whether the presence of the DiI fluorescent label in the DiI-LV formulation could affect drug release, the kinetics of vincristine release from the two formulations was compared in vitro using plasma obtained from NCr-nu athymic mice. As shown in Fig. 1, the in vitro release profiles of DiI-LV and LV were essentially the same with approximately 40% of the encapsulated vincristine released after 26 h of incubation at 37°C.

## Available volume fraction of vincristine

The available volume fraction of VCR (mol. wt. 923) was estimated by $K_{AV}$ of inulin, which was equal to $0.426 \pm 0.037$ (mean ± SD) ($n = 5$) in LX-1 tumors. This was because $K_{AV}$ is insensitive to the molecular weight when it is less than the 5,000 [29]. Thus, the available volume fractions of small molecules are very close to the volume fraction of interstitial fluid space in tissues.

## Tolerability of DiI-LV and LV in mice with window chambers

In both LV- and Dil-LV treated animals, there was moderate body weight loss observed on PTD 2 (6% and 8% for LV and DiI-LV, respectively) and PTD 5 (12% and 10% for LV and DiI-LV, respectively; $P < 0.05$ versus controls). Body weights recovered to near pretreatment levels by PTD 8 (97% and 99% for LV and DiI-LV, respectively). There was no appreciable difference in terms of body weight loss between LV and DiI-LV-treated mice. Tumor-bearing mice that received 0.9% NaCl solution showed slight gain in weight over the 8 days of monitoring.

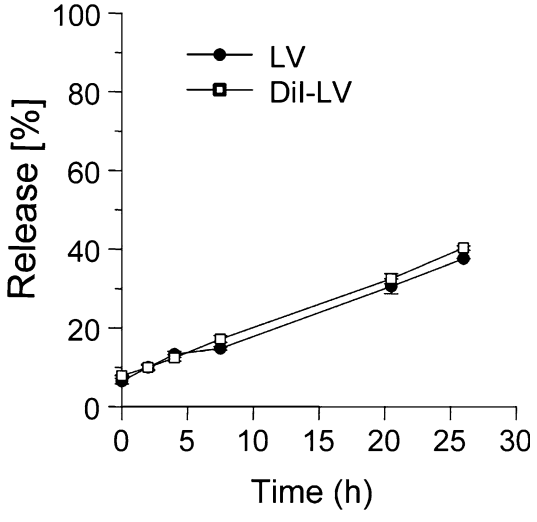


**Fig. 1** Vincristine release from SM/chol liposomes (SM/chol 55/45) in NCr-nu athymic mouse plasma following incubation at 37°C. The lipid concentration was 1.1 mM (0.6 mg/ml) and the drug-to-lipid ratio was 0.05 mg/mg

## Dil-LV extravasation and accumulation in normal and tumor tissues

One to two minutes after DiI-LV i.v. injection, outlines of vessels in normal granulation tissue and tumor tissues were apparent, and the fluorescence was confined to the vessels (Fig. 2a). Extravasation of liposomes was not apparent from vessels of normal granulation tissue in non-tumor windows even 1 h after administration of DiI-LV. In contrast to non-tumor tissue, extravasation of DiI-LV from the tumor irregular and chaotic vasculature into the interstitial tumor spaces was apparent as early as 5 min after drug administration. At 1 h, extensive extravasation was observed (Fig. 2a). DiI-LV accumulated in the perivascular regions of the tumor vessels and overall, showed a punctate pattern of distribution with highest concentrations near vessels.

To quantitate the levels of DiI-LV in the interstitial spaces of normal and tumor tissues, fluorescent images obtained during 1 h after DiI-LV administration were evaluated for relative interstitial amounts (RIA). The results are shown in Fig. 2b. The RIA for DiI-LV was near baseline levels for normal granulation tissue over the course of 1 h. However, the RIA for Dil-LV in tumor tissues continued to increase over the 1 h period of observation. $RIA_{60}$ values for tumor and non-tumor tissues were $0.837 \pm 0.314$ and $0.012 \pm 0.091$, respectively. This difference was significant ($P = 0.01$).

Total fluorescence light intensities were measured in normal granular tissues and tumor tissues from images obtained at 16, 24, and 48 h after administration of DiI-LV. While fluorescence light intensities in normal granulation tissues remained relatively low at all three time points, the light intensities observed in tumor tissues continued to increase over the period of 16 to 48 h. The fluorescence light intensities in tumor tissue were 3.4-, 3.9- and 4.6-fold higher than in normal tissue at 16 , 24 , and 48 h, respectively. The differences between normal tissues and tumor tissues were statistically significant at all three time points ($p < 0.01$, 0.000001, and 0.000001 at 16, 24 and 48 h, respectively); (Fig. 3a).

Images of tumor and adjacent normal tissues showed that the fluorescence was concentrated preferentially within tumor tissues even 5 days after injection (Fig. 3b1). The fluorescence distribution within tumors was heterogeneous. The strongest signal was typically in the perivascular spaces at the tumor periphery. Particularly interesting was the transition of permeability changes of pre-existing host vessels co-opted by growing tumors. As shown in Fig. 3b2 of a relatively small tumor 24 h after DiI-LV injection, remarkable accumulation of

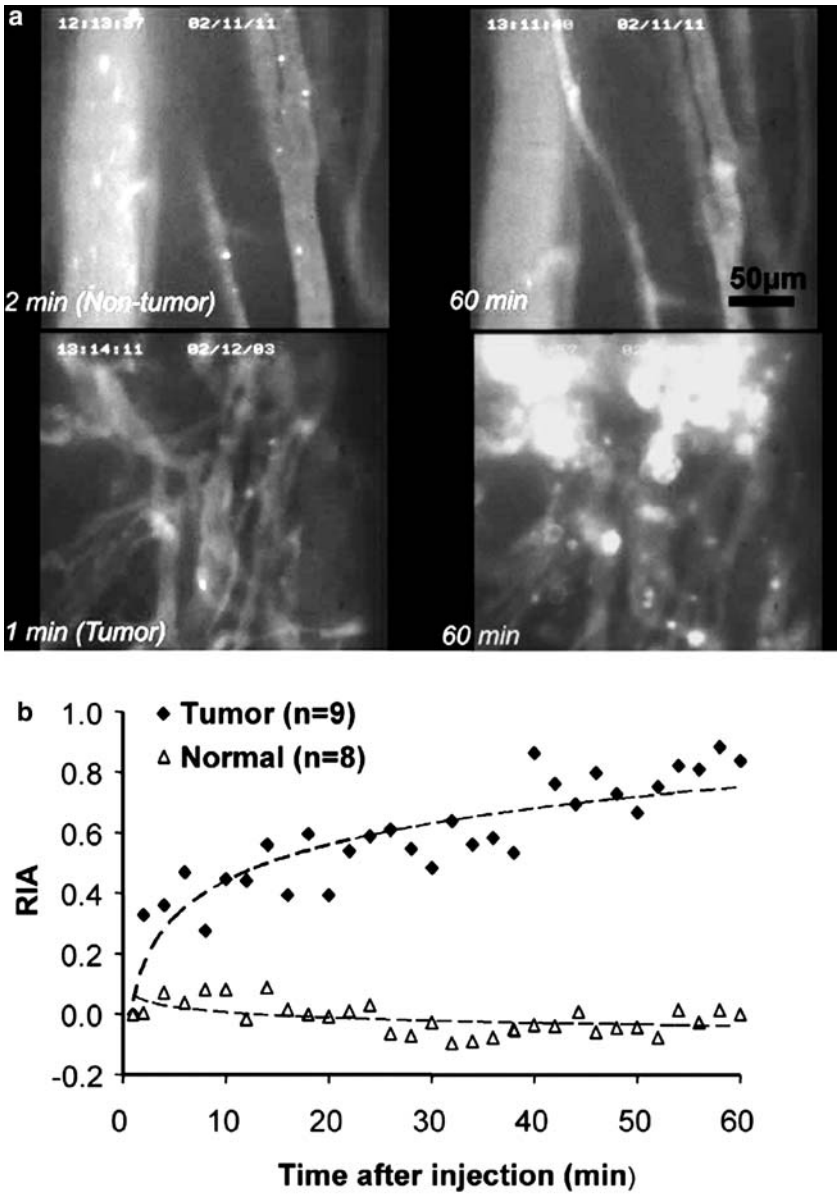


**Fig. 2** Increased extravasation of Dil-LV in tumor vessels. Dil-LV at dose of 1.6 mg/kg was given i.v. and the serial images with intervals of 2 min were recorded after injection over a period of 60 min. Relative interstitial liposome amount (RIA) was calculated from image analysis described in the Materials and Methods. In non-tumor windows little liposome extravasation was observed during 60 min, while extravasation of Dil-LV was readily observed. **a** Examples showing differences in Dil-LV extravasation between normal (*top*) and tumor vessels (*bottom*). Vessel images are sharp and clear after Dil-LV injection with strong fluorescent signal coming from the vasculature, indicating circulation of liposomes. At the end of 60-min experiment, vascular images from normal tissues were still sharp with very little extravasation (*top right*), while in tumor windows many bright spots are seen outside the vessels (*bottom right*). **b** Quantitation of RIA over 60 min after DiI-LV administration. The *trend line* is logarithmic regression

fluorescence was observed from the sections of the pre-existing vessels surrounded by tumor tissues whereas very low levels of accumulation were observed from the regions of the same vessels positioned distally from the tumor tissue.

## Comparison of antitumor activity of DiI-LV and LV in the dorsal skin fold window chamber

The window chamber tumors were monitored for growth following administration of DiI-LV and in a separate group of animals treated with LV. Antitumor activity was monitored up to 8 days after drug administration when tumors could no longer be measured accurately due to tumor tissue outgrowth of the window chamber in the control animals (Fig. 4b insert picture). Both LV and Dil-LV significantly inhibited LX-1 tumor growth (Fig. 4a). Over the 8-day period of observation, LV or Dil-LV-treated tumors did not show growth, whereas 0.9% NaCl solution-treated tumors tripled in tumor area. In addition to the 2D tumor measurements, tumor volumes were also determined on PTD 8 after animals were sacrificed and window chambers were removed. As shown in Fig. 4b, mean tumor volumes in LV-treated mice were less than one-tenth of controls, and Dil-LV-treated tumor volumes were less than one-third of controls. The differences between tumor volumes of either DiI-LV or LV-treated mice relative to the control were statistically significant ($P > 0.001$ and $P > 0.00001$, respectively). Importantly, the slight differences in tumor volumes observed for LV and DiI-LV tumor-bearing animals were not statistically significant ($P > 0.05$).

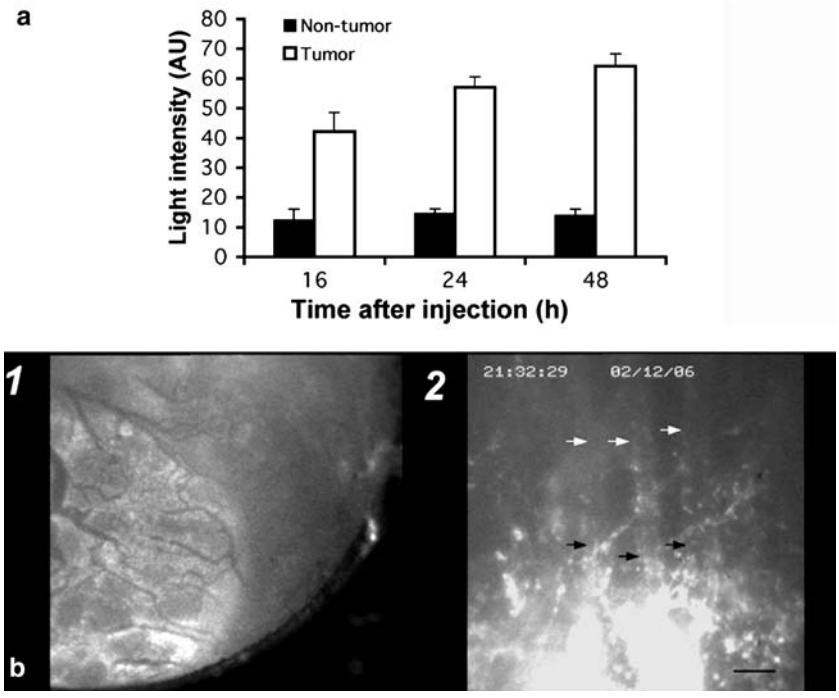


**Fig. 3** Preferential accumulation of Dil-LV in tumor tissue. **a** Fluorescent light intensities were measured in tumor tissue and normal tissues at 16, 24, and 48 h after Dil-LV i.v. injection. Significantly higher accumulation of Dil-LV is seen in tumor tissues. Each column represents mean with SE. $P < 0.01$, 0.000001, 0.000001 at 16, 24, and 48 h, respectively. **b** Examples of DiI-LV tissue distribution. 1 A tumor window showing prolonged accumulation of DiI-LV in tumor tissue. Fluorescence in the tumor remains much higher than in the surrounding non-tumor tissue 5 days after Dil-LV i.v. administration. 2 An example showing the transitional change in vascular permeability to liposomes of coopted vessels induced by tumor growth. The image was taken 24 h after Dil-LV injection. There is clear demonstration of local high permeability in the tumor region, which falls off to background levels in the normal tissue outside the tumor. Segments of three vertical pre-existing vessels near the tumor are indicated by the *black arrows* and segments more distant from the tumor mass are indicated by the *white arrows*. Along the farther distant segments of same vessels, there was almost no liposome accumulation. *Bar*, 50 μm

Tumor areas calculated from digital microscopic images do not measure the thickness of the tumors. For an aggressive tumor cell line, such as LX-1 growing in the chamber with an open skin side, the 2D area measurement likely underestimates the size of the 0.9% NaCl solution-treated control tumors. The relationship between tumor area and tumor volume on PTD 8 is plotted in Fig. 4c. Two dimensional area and 3D volumes correlated linearly when tumor volumes were less than 20 $mm^3$, but as tumor volumes further increased, the tumors tended to expand in the z-direction. Tumor areas on PTD 8 of the majority of LV or DiI-LV treated mice were less than 20 $mm^2$, thus these measurements of tumor areas were fairly accurate. In contrast, tumors in control animals were much larger than 20 $mm^2$ and therefore the difference in treated and control tumor sizes when using area measurements are less than the differences observed using tumor volumes.

## LV exhibits greater antitumor activity than VCR

The window chamber model is not amenable to evaluation of antitumor activity beyond 8 days after drug administration. Therefore, the antitumor activity of LV was evaluated in a flank LX-1 tumor model. LV or VCR was administered at 1.0 mg/kg when tumors were approximately 100 $mm^2$ using a multiple dose schedule of once weekly three times. Figure 5a shows the mean LX-1 tumor volumes over time. Tumor growth time was defined as the days for tumors to attain 1,000 $mm^3$. Weekly administrations of VCR resulted in tumor growth inhibition (growth time were $23.7 \pm 5.3$ vs. $31.2 \pm 5.2$ days for control and VCR, respectively), but the degree of antitumor activity was not statistically significant when compared to control animals. In contrast, administration of LV resulted in prolonged enhancement of tumor growth inhibition ($42.6 \pm 8.6$ days) that was statistically significant when compared to control animals ($P < 0.001$). More importantly, the difference in growth inhibition between LV and VCR was also statistically significant ($P = 0.013$).

## Effects of LV and DiI-LV on tumor vasculature

A moderate reduction of tumor vasculature in window chambers treated with LV and DiI-LV compared with controls was observed. As shown in Fig. 5b VLD values for control animals and animals administered LV and

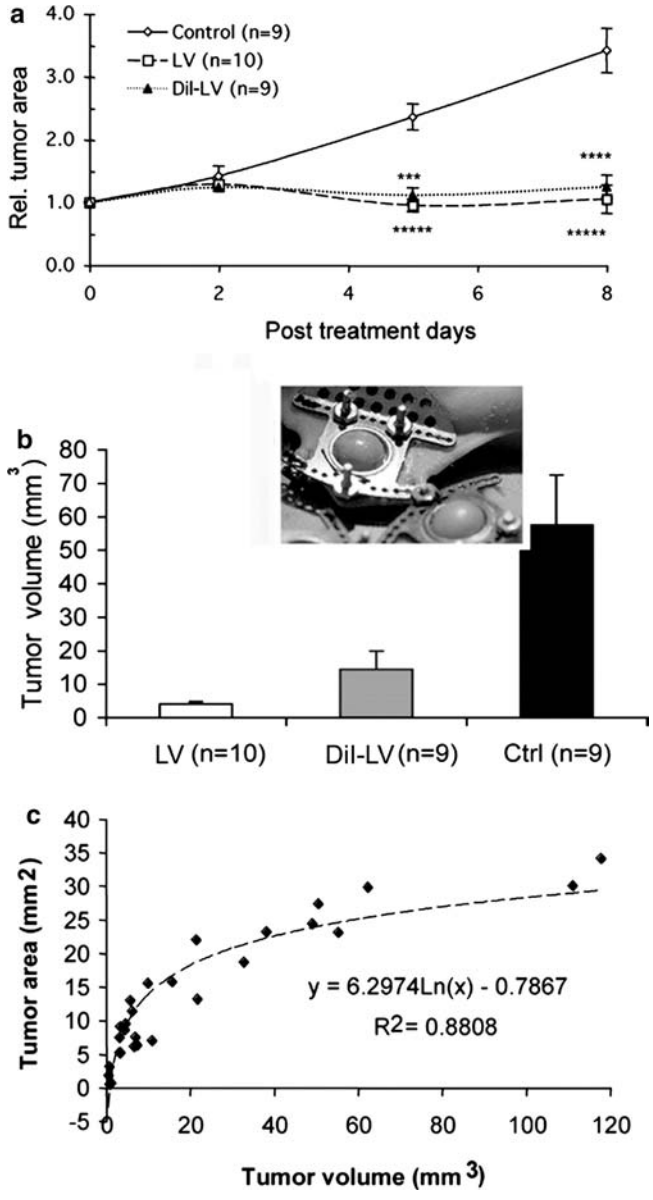


**Fig. 4** Inhibition of tumor growth of LX-1 transplanted in the mouse dorsal skin fold window chambers. A single dose of LV or Dil-LV at 1.6 mg/kg was i.v. administrated on POD 7–11 (PTD 0). Controls received saline only. **a** Tumor areas were measured from images obtained on PTD 0, 2, 5 and 8, and normalized with the areas of PTD 0. *Bars* represent SE, and ***, ****, ***** indicate $P < 0.001$ and $< 0.0001$, and 0.00001, respectively. **b** Tumor volume on PTD 8. $P < 0.01$ between LV and controls, and $P < 0.05$ between DiI-LV and controls. No statistically significant difference was seen between LV and DiI-LV. Seen in the *inserted picture* is tumor growth causing protrusion of the skin on the opposite side from the windows in control mice. LV- and DiI-LV- treated tumors did not show this kind of growth. **c** The relationship between tumor area and tumor volume measurement on PTD 8 is shown. The *trend line* is logarithmic regression

DiI-LV were similar on PTD 0. By PTD 5, the differences in VLD measured between control animals and both liposomal formulations-treated animals were statistically significant. By PTD 8, the differences in VLD measured for control animals and for LV were also statistically significant ($P < 0.05$). Tumor vasculature in LV-treated windows appeared more hemorrhagic with smaller vessel diameters from PTD 5 compared with controls (data not shown).

## Discussion

The capacity of liposomes to extravasate to tumor tissues was evaluated in this study using LV containing the fluorescent lipid marker DiI integrated into the liposomal membrane. Dorsal skin fold window chambers either with or without LX-1 small cell lung tumors were used in conjunction with intravital microscopy to visualize and quantitate extravasation of DiI-LV. These data support the following: (1) DiI-LV extravasation was observed within minutes after drug administration and occurs preferentially from tumor blood vessels as opposed to normal blood vessels; (2) accumulation of DiI-LV in tumor interstitial spaces is approximately 70× greater than in interstitial spaces of normal granulation tissues 1 h after drug administration; (3) DiI-LV accumulates in the perivascular spaces of tumor tissues in a punctate pattern of distribution surrounding tumor microvasculature; and (4) DiI-LV continues to accumulate in tumor tissues for more than 48 h whereas accumulation was not observed in normal granular tissues.

The findings noted earlier for DiI-LV are considered representative of LV based on the following: (1) the liposomes are the same except for the presence of 0.5 mole% DiI; (2) the lipid marker DiI remains associated with the liposome for extended periods in vitro in plasma suggesting that the fluorescent signal observed in vivo was due to DiI incorporated into liposomes and not dissociated DiI; (3) in vitro release of vincristine is similar for LV and DiI-LV; and (4) the toxicity (weight loss) and antitumor activities of DiI-LV and LV were similar.

It was also demonstrated that tumor vascular length densities were less than controls on PTD 5 and 8 in LV-and DiI-LV-treated window chambers. In some tumors, LV caused microhemorrhage around tumor vessels, and in general, the tumor vessel diameters were smaller in LV-treated tumors compared with controls. These results suggest that the drug formulation may have been exhibiting antiangiogenic or vascular damaging effects. Vinca alkaloids, like other tubulin-binding compounds, such as combretastatin A4 [32], have been shown to cause vascular shut down. Vinblastine, a closely similar vinca alkaloid in structure, has shown antivascular and antiangiogenic effects in vitro and in vivo [33–35]. However, until now no studies regarding vascular effects of liposomal VCR have been reported. A study using bFGF-or VEGF-induced mouse corneal neovascularization model showed that VCR at 0.4 mg/kg i.p did not reduce angiogenesis [36]. In another study vincristine at a range of doses (1.0–4.5 mg/kg)

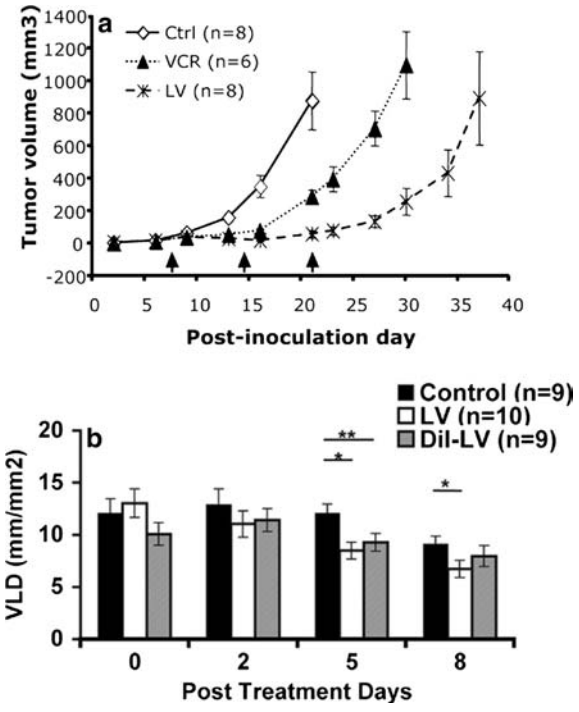


**Fig. 5** **a** Mean tumor volumes of LX-1 tumors grown in the frank s.c. of female NCr-nu athymic mice administered i.v. with weekly doses of LV or VCR. On Days 7, 14, and 21 post-implantation, mice were injected with PBS, 1.0 mg/kg VCR or 1.0 mg/kg LV. *Arrows* on the *x*-axis denote the day of treatment. Data points represent mean ± SE ($n = 6$ or 8). The plot for each treatment group is terminated on the day the first mouse was euthanized due to tumor burden. **b** Tumor VLD as a function of time post-treatment. VLDs were measured from images obtained on PTD 0, 2, 5, and 8. *Bars* represent SE, and *, ** indicate $P < 0.05$ and $< 0.01$, respectively

did not induce a statistically significant inhibition of angiogenesis, and there was no dose-dependent escalation of antiangiogenic effects in a bFGF-induced mouse corneal assay [37]. A recent study, however, showed strong inhibition of VEGF secretion by VCR in the culture media of leukemia cells. It was suggested that inhibition of VEGF may be a mechanism of VCR antileukemic activity, since angiogenesis is believed to be involved in the pathogenesis of hematopoietic malignancies, and VEGF is a critical factor in tumor angiogenesis [38–40]. The observation was limited to 8 days after treatment due to fast growth of LX-1 tumors in window chambers of control animals, therefore, prolonged reduction in subsequent days are nor available. More studies in different tumor models are required. From the trends, it seems that LV demonstrated a slightly stronger inhibitory effect on VLD than DiI-LV, although the differences on all time points were not statistically significant. Similarly, a slightly weaker effect of DiI-LV on tumor volume on PTD 8 was noted (Fig. 4b). Further study is needed to elucidate whether these differences result from tissue distribution disparity between LV and DiI-LV.

The volume available fraction of vincristine in LX-1 tumors was within the range of $K_{AV}$ of other small molecules in tumors reported in the literature [29, 31]. The data indicated that the maximum distribution volume for vincristine was equal to 43% of the total volume in LX-1 tumors. The distribution volume of liposomes should be much smaller than 43% since liposomes accumulate only in perivascular regions. The functions of liposomes in drug delivery are to reduce vincristine accumulation in normal tissues and to form a depot of vincristine in perivascular regions in tumors. As a result, the treatment of tumors relies on vincristine release from liposomes and the subsequent diffusion of vincristine into deeper tissue layers that are inaccessible to liposomes.

In this study the distinct differences in vascular permeability between tumor and normal tissues were shown. Also a transitional change of permeability of pre-existing host vessels from distal to proximal to the growing tumor margin were demonstrated. It clearly indicates that tumor invasion and growth remodels and transforms the pre-existing vessels to more permeable tumor vessels and that these effects are relatively local. In a previous study [41], it was shown that the host vascular remodeling, such as vessel dilation, tortuous changes, and microhemorrhage are the earliest manifestations of tumor-induced angiogenesis. Therefore the remodeling of pre-existing vessels is an essential part of tumor angiogenesis. Tumor vessels are known to have two origins: those vessels formed de novo by sprouting, migration, tubing formation of vascular endothelial cells of the postcapilary venules during growth, and "co-opted" vessels consisting of pre-existing host vessels, which are remodeled by tumor cells during tumor progression. The most likely factors that induce such remodeling are angiogenic growth factors produced by tumor cells, particularly VEGF, a.k.a, vascular permeability factor (VPF). The transitional change along a same pre-existing vessel at different proximity to tumor tissue reflects the gradient of these pro-angiogenic factors from the growing tumors.

Previous studies to characterize the tumor vasculature in pre-clinical animal models mainly employed solid tumor models, however, recent evidence has shown that hematological malignancies also possess abnormal vasculature similar to solid tumors [39, 40, 42]. In diffuse (non-follicular) intermediate-grade and high-grade non-Hodgkin's lymphoma, immature vessels lacking a basement membrane are prevalent [43–45]. Therefore, it is anticipated that extravasation of LV into the interstitial spaces of solid tumors as shown in this report would also occur for tumors of hematological malignancies, such as non-Hodgkin's lymphoma. However, further studies are needed to verify this conjecture. In contrast, extravasation of LV from the vessels of normal tissues was not readily apparent owing to the absence of gaps in the continuous endothelium present in most normal vasculature.

## Conclusion

The liposomes of LV are small, long circulating liposomes with slow release kinetics. These liposomes produce a local depot of encapsulated vincristine in the target tissue and prolong exposure of tumor cells as the drug is slowly released in the tumor interstitial spaces. The preferential extravasation of LV into tumor tissues combined with the enhancement in antitumor activity of LV when compared with VCR as shown in these studies is consistent with the intended design of LV.

**Acknowledgements** The authors thank Ms. Dai Wang for the help in image analysis.

## References

1. Lasic DD, Papahadjopoulos D (1995) Liposomes revisited. Science 267:1275–1276
2. Rahman A, More N, Schein PS (1982) Doxorubicin-induced chronic cardiotoxicity and its protection by liposomal administration. Cancer Res 42:1817–1825
3. Berry G, Billingham M, Alderman E, Torti F, Lum B, DuMond Cea (1996) Reduced cardiotoxicity of Doxil (pegylated liposomal doxorubicin) in aids Kaposi's sarcoma patients compared to a matched control of cancer patients given doxorubicin. Proc Am Soc Clin Oncol 5:A843
4. Muggia F, Hainsworth J, Jeffers S, Miller P, Groshen S, Tan M, et al (1997) Phase ii study of liposomal doxorubicin in refractory ovarian cancer: antitumor activity and toxicity modification by liposomal encapsulation. J Clin Oncol 15:987–993
5. Allen TM, Newman MS, Woodle MC, Mayhew E, Uster PS (1995) Pharmacokinetics and anti-tumor activity of vincristine encapsulated in sterically stabilized liposomes. Int J Cancer 62:199–204
6. Allen TM, Cullis PR (2004) Drug delivery systems: entering the mainstream. Science 303:1818–1822
7. Vaage J, Barberá-Guillem E, Abra R, Huang A, Working P (1994) Tissue distribution and therapeutic effect of intravenous free or encapsulated liposomal doxorubicin on human prostate carcinoma xenografts. Cancer 73:1478–1484
8. Vaage J, Donovan D, Loftus T, Uster P, Working P (1995) Prophylaxis and therapy of mouse mammary carcinomas with doxorubicin and vincristine encapsulated in sterically stabilized liposomes. Eur J Cancer 31A:367–372
9. Abraham SA, Waterhouse DN, Mayer LD, Cullis PR, Madden TD, Bally MB (2005) The liposomal formulation of doxorubicin. Methods in Enzymol 391:71–97
10. Gidding CEM, Kellie SJ, Kamps WA, De Graaf SSN (1999) Vincristine revisited. Crit Rev Oncol Hematol 29:267–287
11. Jackson DVJ, Paschold EH, Spurr CL, Muss HB, Richards FI, Cooper MR, White DR, Stuartt JJ, Hopkins JO, Rich RJ, Wells HB (1984) Treatment of advanced non-Hodgkin's lymphoma with vincristine infusion. Cancer 53:2601–2606
12. Webb MS, Logan P, Kanter PM, St-Onge G, Gelmon K, Harasym T, Mayer LD, Bally MB (1998) Preclinical pharmacology, toxicology and efficacy of sphingomyelin/cholesterol liposomal vincristine for therapeutic treatment of cancer. Cancer Chemother Pharmacol 42:461–470
13. Krishna R, Webb MS, St Onge G, Mayer LD (2001) Liposomal and nonliposomal drug pharmacokinetics after administration of liposome-encapsulated vincristine and their contribution to drug tissue distribution properties. J Pharmacol Exp Ther 298:1206–1212
14. Mayer LD, Bally MB, Loughrey H, Masin D, Cullis PR (1990) Liposomal vincristine preparations which exhibit decreased drug toxicity and increased activity against murine l1210 and p388 tumors. Cancer Res 50:575–579
15. Mayer LD, Nayar R, Thies RL, Boman NL, Cullis PR, Bally MB (1993) Identification of vesicle properties that enhance the antitumor activity of liposomal vincristine against murine l1210 leukemia. Cancer Chemother Pharmacol 33:17–24
16. Mayer LD, Masin D, Nayar R, Boman NL, Bally MB (1995) Pharmacology of liposomal vincristine in mice bearing l1210 ascitic and b16/bl6 solid tumours. Br J Cancer 71:482–488
17. Mayer LD, St-Onge G (1995) Determination of free and liposome-associated doxorubicin and vincristine levels in plasma under equilibrium conditions employing ultrafiltration techniques. Anal Biochem 232:149–157
18. Webb MS, Harasym TO, Masin D, Bally MB, Mayer LD (1995) Sphingomyelin-cholesterol liposomes significantly enhance the pharmacokinetic and therapeutic properties of vincristine in murine and human tumor models. Br J Cancer 72:896–904
19. Webb MS, Saxon D, Wong FM, Lim HJ, Wang Z, Bally MB, Choi LS, Cullis PR, Mayer LD (1998) Comparison of different hydrophobic anchors conjugated to poly (ethylene glycol): effects on the pharmacokinetics of liposomal vincristine. Biochem Biophys Acta 1372:272–282
20. Leonetti C, Scarsella M, Semple SC, Molinari A, D'Angelo C, Stoppacciaro A, Biroccio A, Zupi G (2004) In vivo administration of liposomal vincristine sensitizes drug-resistant human solid tumors. Int J Cancer 110:767–774
21. Fiske CH, Subbarow Y (1925) The colorimetric determination of phosphorus. J Biol Chem 66:375–400
22. Fenske DB, Maurer N, Cullis PR (2003) Liposomes: a practical approach. In: Torchilin VP, Weissig V (eds) Oxford University Press, Oxford, New York, pp. 167–191
23. Venditti JM, Wesley RA, Plowman J (1984) Current NCI preclinical antitumor screening in vivo: results of tumor panel screening, 1976–1982, and future directions. Adv Pharmacol Chemother 20:1–20
24. Tashiro T, Inaba M, Kobayashi T, Sakurai Y, Maruo K, Ohnishi Y, Ueyama Y, Nomura T (1989) Responsiveness of human lung cancer/nude mouse to antitumor agents in a model using clinically equivalent doses. Cancer Chemother Pharmacol 24:187–192
25. Huang Q, Shan S, Braun RD, Lanzen J, Anyrhambatla G, Kong G, Borelli M, Corry P, Dewhirst MW, Li CY (1999) Noninvasive visualization of tumors in rodent dorsal skin window chambers. Nat Biotechnol 17:1033–1035
26. Shan S, Lockhart AC, Saito WY, Knapp AM, Laderoute KR, Dewhirst MW (2001) The novel tubulin-binding drug bto-956 inhibits r3230ac mammary carcinoma growth and angiogenesis in Fischer 344 rats. Clin Cancer Res 7:2590–2596
27. Wu NZ, Klitzman B, Rosner GL, Needham D, Dewhirst MW (1993) Measurement of material extravasation in microvascular networks using fluorescence video-microscopy. Microvasc Res 46:231–253
28. Kong G, Braun RD, Dewhirst MW (2000) Hyperthermia enables tumor-specific nanoparticle delivery: effect of particle size. Cancer Res 60:4440–4445
29. Krol A, Maresca J, Dewhirst MW, Yuan F (1999) Available volume fraction of macromolecules in the extravascular space of a fibrosarcoma: implications for drug delivery. Cancer Res 59:4136–4141
30. Yuan F, Krol A, Tong S (2001) Available space and extracellular transport of macromolecules: effects of pore size and connectedness. Ann Biomed Eng 29:1150–1158
31. Krol A, Dewhirst MW, Yuan F (2003) Effects of cell damage and glycosaminoglycan degradation on available extravascular space of different dextrans in a rat fibrosarcoma. Int J Hyperthermia 19:154–164
32. Siemann DW, Chaplin D, Horsman MR (2004) Vascular-targeting therapies for treatment of malignant disease. Cancer 100:2491–2499

33. Vacca A, Iurlaro M, Ribatti D, Minischetti M, Nico B, Ria R, Pellegrino A, Dammacco F (1999) Antiangiogenesis is produced by nontoxic doses of vinblastine. Blood 94:4143–4155
34. Hill SA, Lonergan SJ, Denekamp J, Chaplin DJ (1993) Vinca alkaloids: Anti-vascular effects in a murine tumor. Eur J Cancer 29:1320–1324
35. Schirner M, Hoffmann J, Menrad A, Schneider M (1998) Antiangiogenic chemotherapeutic agents: characterization in comparison to their tumor growth inhibition in human renal cell carcinoma models. Clin Cancer Res 4:1331–1336
36. Klauber N, Parangi S, Flynn E, Hamel E, D'Amato RJ (1997) Inhibition of angiogenesis and breast cancer in mice by the microtubule inhibitors 2-methoxyestradiol and Taxol. Cancer Res 57:81–86
37. O'Leary JJ, Shapiro RL, Ren CJ, Chuang N, Cohen HW, Potmesil M (1999) Antiangiogenic effects of camptothecin analogues 9-amino-20(s)-camptothecin, topotecan, and cpt-11 studied in the mouse cornea model. Clin Cancer Res 5:181–187
38. Avramis IA, Kwock R, Avramis VI (2001) Taxotere and vincristine inhibit the secretion of the angiogenesis inducing vascular endothelial growth factor (VEGF) by wild-type and drug-resistant human leukemia t-cell lines, Anticancer Res 21:2281–2286
39. Moehler T, Neben K, Ho A, Goldschmidt H (2001) Angiogenesis in hematologic malignancies. Ann Hemotol 80:695–705
40. Orpana A, Salven P (2002) Angiogenic and lymphangiogenic molecules in hematological malignancies. Leuk Lymphoma 43:219–224
41. Carmeliet P, Jain RK (2000) Angiogenesis in cancer and other diseases. Nature 407:249–257
42. Salven P (2001) Angiogenesis in lymphoproliferative disorders. Acta Haematol 106:184–189
43. Vacca A, Ribatti D, Roncali L, Dammacco F (1995) Angiogenesis in b cell lymphoproliferative diseases. Biological and clinical studies. Leuk Lymphoma 20:27–38
44. Ribatti D, Vacca A, Nico B, Fanelli M, Roncali L, Dammacco F (1996) Angiogenesis spectrum in the stroma of b-cell non-Hodgkin's lymphomas. An immunohistochemical and ultrastructural study. Eur J Haematol 56:45–53
45. Ribatti D, Vacca A, Marzullo A, Nico B, Ria R, Roncali L, Dammacco F (2000) Angiogenesis and mast cell density with tryptase activity increase simultaneously with pathological progression in b-cell non-Hodgkin's lymphomas. Int J Cancer 85:171–175